Three-pathway electromagnetically induced transparency in coupled-cavity optomechanical system

Fu-Chuan Lei,[1,2] **Ming Gao,**[1,2] **Chunguang Du,**[1,2] **Qing-Li Jing**[1,2], **and Gui-Lu Long**[1,2,3]*

[1]*State Key Laboratory of Low-dimensional Quantum Physics and Department of Physics, Tsinghua University, Beijing 100084, China*

[2]*Tsinghua National Laboratory of Information Science and Technology, Beijing 100084, China*

[3]*Collaborative Innovation Center of Quantum Matter, Beijing 100084, China*

*gllong@tsinghua.edu.cn

Abstract: Recently Qu and Agarwal [Phys Rev. A. **22**, 031802 (2013)] found a three-pathway electromagnetically induced absorption (TEIA) phenomenon within a mechanically coupled two-cavity system, where there exist a sharp EIA dip in the broad electromagnetically induced transparency peak in the transmission spectrum. In this work, we study the response of a probe light in a pair of directly coupled microcavities with one mechanical mode. We find that in addition to the sharp TEIA dip within a broad EIT window as found by Qu and Agarwal, three-pathway electromagnetically induced transparency (TEIT) within the broad EIT window could also exist under certain conditions. We give explicit physical explanations and detailed calculations. Our results provide a method for controlling transition between TEIA and TEIT in coupled optomechanical systems, and reveal the multiple pathways interference is versatile for controlling light.

OCIS codes: (120.4880) Optomechanics; (020.3690) Line shapes and shifts; (140.3945) Microcavities; (270. 1670) Coherent optical effects.

References and links

1. S. E. Harris, "Electromagnetically induced transparency," Phys. Today **50**, 36–42 (1997).
2. S. E. Harris, J. E. Field, and A. Imamoğlu, "Nonlinear optical processes using electromagnetically induced transparency," Phys. Rev. Lett. **64**, 1107–1110 (1990).
3. K.-J. Boller, A. Imamolu, and S. E. Harris, "Observation of electromagnetically induced transparency," Phys. Rev. Lett. **66**, 2593–2596 (1991).
4. M. Fleischhauer, A. Imamoglu, and J. P. Marangos, "Electromagnetically induced transparency: Optics in coherent media," Rev. Mod. Phys. **77**, 633–673 (2005).
5. U. Fano, "Effects of configuration interaction on intensities and phase shifts," Phys. Rev. **124**, 1866–1878 (1961).
6. A. E. Miroshnichenko, S. Flach, and Y. S. Kivshar, "Fano resonances in nanoscale structures," Rev. Mod. Phys. **82**, 2257–2298 (2010).
7. S. Fan, W. Suh, and J. Joannopoulos, "Temporal coupled-mode theory for the fano resonance in optical resonators," J. Opt. Soc. Am. A **20**, 569–572 (2003).
8. F. Lei, B. Peng, Ş. K. Özdemir, G. L. Long, and L. Yang, "Dynamic fano-like resonances in erbium-doped whispering-gallery-mode microresonators," Appl. Phys. Lett. **105**, 101112 (2014).
9. L. Hau, S. E. Harris, Z. Dutton, and C. H. Behroozi, "Light speed reduction to 17 metres per second in an ultracold atomic gas," Nature **397**, 594–598 (1999).
10. C. Liu, Z. Dutton, C. H. Behroozi, and L. Hau, "Observation of coherent optical information storage in an atomic medium using halted light pulses," Nature **409**, 490–493 (2001).

#234484 - $15.00 USD Received 24 Feb 2015; revised 21 Mar 2015; accepted 22 Mar 2015; published 23 Apr 2015

11. M. D. Lukin, "*Colloquium* : Trapping and manipulating photon states in atomic ensembles," Rev. Mod. Phys. **75**, 457–472 (2003).
12. S. Zhang, D. A. Genov, Y. Wang, M. Liu, and X. Zhang, "Plasmon-induced transparency in metamaterials," Phys. Rev. Lett. **101**, 047401 (2008).
13. N. Papasimakis, V. A. Fedotov, N. I. Zheludev, and S. L. Prosvirnin, "Metamaterial analog of electromagnetically induced transparency," Phys. Rev. Lett. **101**, 253903 (2008).
14. P. Tassin, L. Zhang, T. Koschny, E. N. Economou, and C. M. Soukoulis, "Low-loss metamaterials based on classical electromagnetically induced transparency," Phys. Rev. Lett. **102**, 053901 (2009).
15. S. E. Harris, "Electromagnetically induced transparency in an ideal plasma," Phys. Rev. Lett. **77**, 5357–5360 (1996).
16. E. Kawamori, W.-J. Syugu, T.-Y. Hsieh, S.-X. Song, and C. Z. Cheng, "Experimental identification of electromagnetically induced transparency in magnetized plasma," Phys. Rev. Lett. **108**, 075003 (2012).
17. G. Shvets and A. Pukhov, "Electromagnetically induced guiding of counterpropagating lasers in plasmas," Phys. Rev. E **59**, 1033–1037 (1999).
18. T. Wang, Y. Zhang, Z. Hong, and Z. Han, "Analogue of electromagnetically induced transparency in integrated plasmonics with radiative and subradiant resonators," Opt. Express **22**, 21529–21534 (2014).
19. D. D. Smith, H. Chang, K. A. Fuller, A. T. Rosenberger, and R. W. Boyd, "Coupled-resonator-induced transparency," Phys. Rev. A **69**, 063804 (2004).
20. A. Naweed, G. Farca, S. I. Shopova, and A. T. Rosenberger, "Induced transparency and absorption in coupled whispering-gallery microresonators," Phys. Rev. A **71**, 043804 (2005).
21. K. Totsuka, N. Kobayashi, and M. Tomita, "Slow light in coupled-resonator-induced transparency," Phys. Rev. Lett. **98**, 213904 (2007).
22. B. Peng, Ş. K. Özdemir, W. Chen, F. Nori, and L. Yang, "What is and what is not electromagnetically induced transparency in whispering-gallery microcavities," Nat. Comm. **5**, 5082 (2014).
23. A. Naweed, D. Goldberg, and V. M. Menon, "All-optical electromagnetically induced transparency using one-dimensional coupled microcavities," Opt. Express **22**, 18818–18823 (2014).
24. G. S. Agarwal and S. Huang, "Electromagnetically induced transparency in mechanical effects of light," Phys. Rev. A **81**, 041803 (2010).
25. S. Weis, R. Rivière, S. Deléglise, E. Gavartin, O. Arcizet, A. Schliesser, and T. J. Kippenberg, "Optomechanically induced transparency," Science **330**, 1520–1523 (2010).
26. J. D. Teufel, D. Li, M. Allman, K. Cicak, A. Sirois, J. Whittaker, and R. Simmonds, "Circuit cavity electromechanics in the strong-coupling regime," Nature **471**, 204–208 (2011).
27. P.-C. Ma, J.-Q. Zhang, Y. Xiao, M. Feng, and Z.-M. Zhang, "Tunable double optomechanically induced transparency in an optomechanical system," Phys. Rev. A **90**, 043825 (2014).
28. C. G. Alzar, M. Martinez, and P. Nussenzveig, "Classical analog of electromagnetically induced transparency," Am. J. Phys. **70**, 37–41 (2002).
29. K. Qu and G. S. Agarwal, "Phonon-mediated electromagnetically induced absorption in hybrid opto-electromechanical systems," Phys. Rev. A **87**, 031802 (2013).
30. Y. He, "Optomechanically induced transparency associated with steady-state entanglement," Phys. Rev. A **91**, 013827 (2015).
31. I. S. Grudinin, H. Lee, O. Painter, and K. J. Vahala, "Phonon laser action in a tunable two-level system," Phys. Rev. Lett. **104**, 083901 (2010).
32. M. Bayer, T. Gutbrod, J. P. Reithmaier, A. Forchel, T. L. Reinecke, P. A. Knipp, A. A. Dremin, and V. D. Kulakovskii, "Optical modes in photonic molecules," Phys. Rev. Lett. **81**, 2582–2585 (1998).
33. B. Peng, Ş. K. Özdemir, J. Zhu, and L. Yang, "Photonic molecules formed by coupled hybrid resonators," Opt. Lett. **37**, 3435–3437 (2012).
34. B. Peng, Ş. K. Özdemir, F. Lei, F. Monifi, M. Gianfreda, G. L. Long, S. Fan, F. Nori, C. M. Bender, and L. Yang, "Parity-time-symmetric whispering-gallery microcavities," Nat. Physics **10**, 394–398 (2014).
35. T. Carmon, H. Rokhsari, L. Yang, T. J. Kippenberg, and K. J. Vahala, "Temporal behavior of radiation-pressure-induced vibrations of an optical microcavity phonon mode," Phys. Rev. Lett. **94**, 223902 (2005).
36. M. Gao, F.-C. Lei, C.-G. Du, and G.-L. Long, "Self-sustained oscillation and dynamical multistability of optomechanical systems in the extremely-large-amplitude regime," Phys. Rev. A **91**, 013833 (2015).
37. L. Zhang and Z. Song, "Modification on static responses of a nano-oscillator by quadratic optomechanical couplings," Sci China- Phys Mech Astron **57**, 880–886 (2014).
38. W. Nie, Y. Lan, Y. Li, and S. Zhu, "Generating large steady-state optomechanical entanglement by the action of casimir force," Sci China- Phys Mech Astron **57**, 2276–2284 (2014).
39. H. Xiong, L.-G. Si, A.-S. Zheng, X. Yang, and Y. Wu, "Higher-order sidebands in optomechanically induced transparency," Phys. Rev. A **86**, 013815 (2012).
40. M. Cai, O. Painter, and K. J. Vahala, "Observation of critical coupling in a fiber taper to a silica-microsphere whispering-gallery mode system," Phys. Rev. Lett. **85**, 74–77 (2000).
41. P. Anisimov and O. Kocharovskaya, "Decaying-dressed-state analysis of a coherently driven three-level λ system," J. Mod. Opt. **55**, 3159–3171 (2008).

#234484 - $15.00 USD Received 24 Feb 2015; revised 21 Mar 2015; accepted 22 Mar 2015; published 23 Apr 2015

42. J. M. Dobrindt, I. Wilson-Rae, and T. J. Kippenberg, "Parametric normal-mode splitting in cavity optomechanics," Phys. Rev. Lett. **101**, 263602 (2008).
43. S. Gröblacher, K. Hammerer, M. R. Vanner, and M. Aspelmeyer, "Observation of strong coupling between a micromechanical resonator and an optical cavity field," Nature **460**, 724–727 (2009).
44. F. Lei, M. Gao, C. Du, S.-Y. Hou, X. Yang, and G. L. Long, "Engineering optomechanical normal modes for single-phonon transfer and entanglement preparation," J. Opt. Soc. Am. B **32**, 588–594 (2015).

1. Introduction

Multiple pathways interference plays a fundamental role in classical and quantum physics, which yields many novel coherent phenomena. A typical example in optics is electromagnetically induced transparency (EIT) [1–4]. EIT originates from Fano interference [5–8] between two excitation pathways to the internal upper level of atoms. Due to the opposite phases of the two transition amplitudes, the absorption is cancelled and a sharp transparent peak occurs at the resonant frequency of a transition. Besides, this type of destructive interference also gives rise to an extreme dispersion within the transparent window, which is widely exploited to produce slow light [9], store light pulses [10] and generate giant nonlinear effects even at the single-photon level [11]. EIT is not an exclusive phenomenon in quantum mechanics, and it also exists widely in classical systems. The only difference between quantum and classical EIT is that the former is described by probability amplitude while the latter is by field, but they have the property of interference in common.

In recent years, there is an increasing interest in implementating EIT in a variety of classical artificial systems because they are more easily to control and have wide applications, such as in metamaterials [12–14], plasma [15–18], microcavities [19–23], and optomechanics [24–27]. The systems of the EIT mentioned above can be generally attributed to two coupled harmonic oscillators [28] with distinct quality (Q) factors. For example, the coupled-resonator-induced transparency (CRIT) describes that, a high Q cavity mode and a low Q one are weakly coupled, resulting in a cancellation of absorption at their original resonant frequency. In optomechanically induced transparency (OMIT) scenario, a high Q mechanical resonator is coupled with a cavity mode driven by a red-detuned pump field. This modulated cavity mode has an effective resonant frequency close to that of the mechanical resonator while its effective Q factor is low. At present, most studies of EIT focus on the systems which can be understood in terms of two coupled oscillators. It is essentially equivalent to two pathways interference. However, a natural generalization of the two oscillators model to three or even more may bring about novel coherent effects since more transition pathways are involved for the probe. This generalized model may provide a good platform to investigate the physics of multiple pathways interference and simulate some complicated quantum coherent effects [29, 30]. For instance, recently Qu and Agarwal reported the existence of the three-pathway electromagnetically induced absorption (TEIA) phenomenon in the double-cavity configuration of the hybrid opto-electromechanical systems [29]. In their work, one more microwave cavity mode is introduced to couple with the mechanical mode in the standard optomechanical system. The new cavity mode provides an additional pathway and it can break the original destructive interference, which can result in absorption instead of transparency at the resonance.

In this paper, we consider a similar three-mode configuration: two coupled cavity modes and one mechanical mode, while only one cavity mode interacts with the mechanical mode by radiation pressure. The model essentially involves two types of mechanisms to induce transparency at the resonant frequency of a cavity mode, i.e., CRIT and OMIT. Then one may ask a natural question: whether the transparent peak will become higher under their combined effects? The answer is not simple, because their interaction is coherent. The combination of the two mechanisms can offer rich interesting modulation for probe light. We will show that the system can not only produce three-pathway electromagnetically induced absorption (TEIA) but also trans-

#234484 - $15.00 USD Received 24 Feb 2015; revised 21 Mar 2015; accepted 22 Mar 2015; published 23 Apr 2015

parency (TEIT) within a relatively wide transparent window over a wide range of parameters. We discuss the origin of the TEIA and TEIT. A criterion for TEIA and TEIT is given, which fits well with the exact numerical calculations.

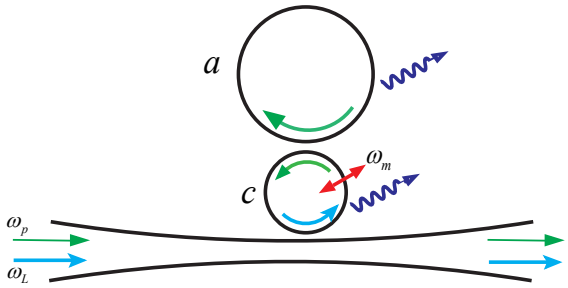

Fig. 1. The schematic of the considered system. Two WGM microcavities (a and c) are directly coupled by evanescent field. Cavity c contains a mechanical mode with frequency ω_m. A fiber taper waveguide is side-coupled to cavity c for light input and output. Two laser fields with frequencies ω_L and ω_p are input to drive and probe the system, respectively.

2. Model

The schematic of the system we consider is shown in Fig. 1. Similar to the previously reported phonon laser structure [31], it is formed by coupling two Whispering-Gallery-Mode (WGM) microcavities (a and c), which is sometimes called photonic molecule [32] and is widely reported for different applications [33, 34]. One of the two cavities is coupled to a waveguide by evanescent field for coupling light into and out of the system. The Hamiltonian of our proposed system is given by

$$\begin{aligned} H &= H_0 + H_c + H_I + H_d, \\ H_0 &= \hbar\omega_c c^\dagger c + \hbar\omega_a a^\dagger a + \frac{p^2}{2m} + \frac{1}{2}m\omega_m^2 q^2, \\ H_c &= \hbar\lambda(ac^\dagger + ca^\dagger), \\ H_I &= \hbar g c^\dagger c q, \\ H_d &= i\hbar\varepsilon_L(c^\dagger e^{-i\omega_L t} - ce^{i\omega_L t}) + i\hbar\varepsilon_p(c^\dagger e^{-i\omega_p t} - ce^{i\omega_p t}), \end{aligned} \tag{1}$$

where c ($c^\dagger$) and a ($a^\dagger$) denote the cavity annihilation (creation) operators for the two WGM microcavities. They are coupled by evanescent field with strength λ. Assuming the c cavity supports a low threshold mechanical mode b, which is described by a harmonic oscillator with effective mass m, frequency ω_m. The cavity mode c and the mechanical mode b are dispersively coupled via radiation pressure and the coupling strength is g. A pump field and a probe field are introduced with frequencies ω_L and ω_p to the cavity mode c. In Eq. (1), $\varepsilon_L = \sqrt{2\kappa_{ex}P_L/\hbar\omega_L}$, and $\varepsilon_p = \sqrt{2\kappa_{ex}P_p/\hbar\omega_p}$, where P_L is the pump power, P_p is the probe power, κ_{ex} is the coupling loss of cavity mode c to waveguide.

In this work, we study the response of the system to a classical probe, which is strong enough compared to single photons but much weaker than the pump field. Therefore, the quantum fluctuations can be averaged to zero, and the operators can be treated as c-numbers. In the

#234484 - $15.00 USD Received 24 Feb 2015; revised 21 Mar 2015; accepted 22 Mar 2015; published 23 Apr 2015

rotating frame at the frequency ω_L of the pump field, we can obtain the Langevin equations of the system by adding damping terms,

$$\begin{aligned}
\frac{dq}{dt} &= \frac{p}{m}, \\
\frac{dp}{dt} &= -m\omega_m^2 q - \hbar g c^\dagger c - \gamma_m p, \\
\frac{dc}{dt} &= -[\kappa_c + i(\omega_c - \omega_L + gq)]c + \varepsilon_L - i\lambda a + \varepsilon_p e^{-i\delta t}, \\
\frac{da}{dt} &= -[\kappa_a + i(\omega_a - \omega_L)]a - i\lambda c,
\end{aligned} \tag{2}$$

where $\delta = \omega_p - \omega_L$, γ_m is the damping rate of the mechanical mode. κ_c is the sum of intrinsic and coupling loss (to waveguide) for cavity mode c. κ_a denotes the intrinsic loss of cavity mode a. We assume that there is no loss for the coupling of the two caviy modes or the loss is constant so it can be included in their intrinsic loss. If the applied pump power is beyond a critical point, the mechanical mode will start to oscillate and the system becomes unstable [35–38]. We limit our study to the stable driving regime. To get the stable condition, we can linearize the above coupled equations [Eq. (2)] to the first order of the probe. To perform it, we decompose each observable O by $O_0 + \delta O$, where O_0 and δO stand for the quantity of the zero and first order of probe, respectively. Assuming our system is in the resolved sideband regime, we can neglect the high order sideband effect [39] and focus on the dynamics of the first order quantities, which determines the response of the considered system to probe. After a short calculation, the following Langevin equations can be obtained to describe their motion,

$$\frac{dX}{dt} = DX + \zeta \tag{3}$$

where, $X = [\ \delta q \quad \delta p \quad \delta c \quad \delta a \quad \delta c^* \quad \delta a^*\ ]^T$,

$$D = \begin{pmatrix}
0 & \frac{1}{m} & 0 & 0 & 0 & 0 \\
-m{\omega_m}^2 & -\gamma_m & -\hbar g {c_0}^* & 0 & -\hbar g c_0 & 0 \\
-igc_0 & 0 & -(\kappa_c + i\Delta_c) & -i\lambda & 0 & 0 \\
0 & 0 & -i\lambda & -(\kappa_a + i\Delta_a) & 0 & 0 \\
igc_0{}^* & 0 & 0 & 0 & -(\kappa_c - i\Delta_c) & i\lambda \\
0 & 0 & 0 & 0 & i\lambda & -(\kappa_a - i\Delta_a)
\end{pmatrix},$$

$\zeta = \left[\ 0 \quad 0 \quad \varepsilon_p e^{-i\delta t} \quad 0 \quad {\varepsilon_p}^* e^{i\delta t} \quad 0\ \right]^T$, $\Delta_c = \omega_c - \omega_L + gq_0$ and $\Delta_a = \omega_a - \omega_L$, c_0, a_0, and q_0 can be easily obtained from the coupled steady state equations according to Eq. (2). The stability is determined by the maximum real part of all the eigenvalues of the above 6×6 evolution matrix D. If it is negative, then the system is stable, otherwise, it is unstable.

We can use the following ansatz to express the fluctuation parts of cavity field a, c, and the displacement of the mechanical mode ,

$$\begin{aligned}
\delta c &= c_+ e^{-i\delta t} + c_- e^{i\delta t}, \\
\delta a &= a_+ e^{-i\delta t} + a_- e^{i\delta t}, \\
\delta q &= q_+ e^{-i\delta t} + q_- e^{i\delta t}.
\end{aligned} \tag{4}$$

We introduce a function $R(\delta)$ to describe the response for the probe light, and it is defined as $R(\delta) = c_{out}(\delta)/c_{in}(\delta)$, where c_{out} and c_{in} denote the output and input amplitude at the frequency of the probe, respectively. Using input-output relations we can obtain $R(\delta) = \eta\varepsilon_T -$

#234484 - $15.00 USD Received 24 Feb 2015; revised 21 Mar 2015; accepted 22 Mar 2015; published 23 Apr 2015

1, where η is defined as the radio between the coupling loss κ_{ex} and the total loss κ_c, and ε_T equals to $2\kappa_c c_+ \big/ \varepsilon_p$. Without loss of generality, we assume the waveguide and the cavity c is critically coupled [40], which means $\eta = 1/2$. After detailed derivation we get

$$R(\delta) = 2\kappa_c \frac{X(\delta)\Lambda(\delta) + i\beta\Lambda(\delta)\Lambda^*(-\delta))}{X(\delta) - i\beta(\Lambda(\delta) - \Lambda^*(-\delta))} - 1, \tag{5}$$

where $X(\delta) = -\delta^2 + {\omega_m}^2 - i\delta\gamma_m$, $\beta = \hbar g^2 |c_0|^2 \big/ m$ and $\Lambda(\delta) = \{[\kappa_c + i(\Delta_c - \delta)] + \lambda^2 \big/ [\kappa_a + i(\Delta_a - \delta)]\}^{-1}$.

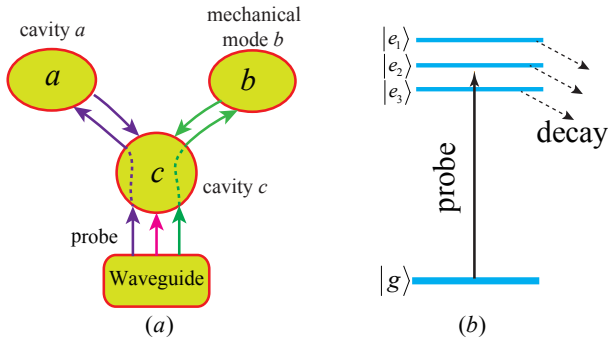

Fig. 2. Illustration of the three-pathway interference (a) in the real pathway picture and (b) in the decaying-normal-mode picture.

3. TEIT and TEIA

Before the detailed calculation, we will briefly discuss the physical origins of TEIT and TEIA in our model. As we mentioned, to produce EIT or EIA, we need two pathways that interference. OMIT and CRIT are exactly these cases. Compared to them, one more pathway is introduced in our model. Therefore, there exist three possible mechanisms to excite the cavity mode c. As shown in Fig. 2(a), they are: (1) direct coupling the probe light from waveguide into the cavity; (2) coupling the probe light from waveguide via cavity a (the pathway of light is: waveguide $\longrightarrow$ cavity c $\longrightarrow$ cavity a $\longrightarrow$ cavity c, which is similar to EIT in atoms, one of the transition path is: one lower state $\longrightarrow$ excited state $\longrightarrow$ another lower state $\longrightarrow$ excited state); (3) coupling light due to the anti-Stokes process of optomechanical interaction (probe light and pump field cooperate to produce phonons in mechanical mode, and the produced phonons and pump field can reproduce a field with frequency close to cavity mode c). The interference of the three pathways may lead to the diverse resonant structures depending on their amplitudes and relative phases. Inspired by using decaying-dressed states to interpret EIT in atoms [41], we can also treat the three-pathway interference in decaying-normal-mode picture (or growing-normal-mode, depending on the sign of the decay rates of the three normal modes). This can gives a more simple interpretation and classification of various coherent effects for our model. The three decaying-normal-modes are obtained from decoupling the three coupled bare modes. Hence, it can be considered that our system provides three resonant modes or three resonant excitation pathways for the probe field. As shown in Fig. 2(b), the system can be considered as an analog of four-level system, the three excited levels have different decay rates which is equivalent to that the Q factors of the three normal modes are different. The three excitation pathways may interference, resulting in a variety of transmission spectra such as TEIA or TEIT.

#234484 - $15.00 USD Received 24 Feb 2015; revised 21 Mar 2015; accepted 22 Mar 2015; published 23 Apr 2015

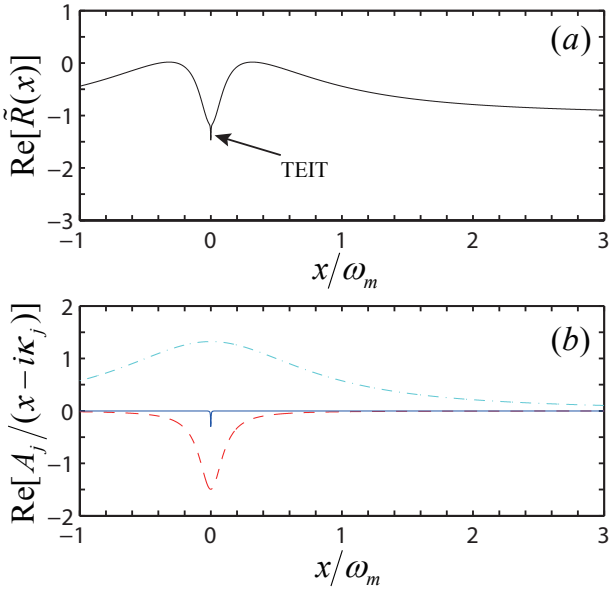

Fig. 3. The real parts of (a) the response function $\widetilde{R}(x)$ and (b) its three normal modes compenents. Here $\lambda = 0.1\omega_m$, $\beta = 0.2{\omega_m}^3$, $\kappa_c = \omega_m$, $\gamma_m = 10^{-3}\omega_m$, $\kappa_a = 5\gamma_m$, corresponding to the black point in area T of Fig. 5. It shows that the optomechanical interaction produces a more sharp TEIT peak within the CRIT window.

In order to get more insight into the system, we need to deal with Eq. (5). It is shown that under certain conditions, the complicated expression of $R(\delta)$ can be reduced to a simpler form $\widetilde{R}(\delta)$. We set $\delta \sim \omega_m \simeq \Delta_c = \Delta_a$ to enable the optomechanical interaction to be the strongest. To make the linewidth of TEIT peak or TEIA dip narrow enough, we assume $\omega_m \sim \kappa_c \gg \kappa_a, \gamma_m$, then we get

$$\widetilde{R}(x) = \frac{\kappa_c}{(\kappa_c - ix) + \frac{\lambda^2}{\kappa_a - ix} + \frac{\beta/2\omega_m}{\kappa_m - ix}} - 1, \tag{6}$$

where $x = \delta - \omega_m$ and $\kappa_m = \gamma_m/2 - \kappa_c\beta/[2\omega_m({\kappa_c}^2 + 4{\omega_m}^2)]$. This approximate expression $\widetilde{R}(x)$ has been confirmed by numerical comparison with its exact formula [Eq.(5)]. The structure of $\widetilde{R}(x)$ is very interesting. It shows that how the resonant character of the output field changes from an empty cavity ($\lambda = \beta = 0$) to the CRIT case ($\beta = 0$) or OMIT case ($\lambda = 0$) as well as the general case ($\lambda \neq 0, \beta \neq 0$). The response of the system is determined by the two parameters, i.e., coupling coefficient λ and driving coefficient β, which characterize the strength of CRIT and OMIT, respectively.

To illustrate how λ and β affect the output fields, we can set $x = 0$ to examine how $\widetilde{R}(0)$ varies with them. When $\beta = 0$, $\widetilde{R}(0)$ will decrease with λ increasing because λ^2/κ_a is always positive. Therefore, once a nonzero λ is introduced, a transparent peak will emerge within the broad absorption dip in transmission spectra, which is known as CRIT. If $\beta \neq 0$ and κ_m is positive, the third term of the denominator of $\widetilde{R}(x)$ will contribute similarly to the second term, which will further decrease $\widetilde{R}(0)$, resulting in the emergence of a new transparent peak within the above mentioned CRIT peak. As we stated before, this new peak is TEIT peak because it results from three-pathway interference. In Fig. 3(a), we plot the real part of the

#234484 - $15.00 USD Received 24 Feb 2015; revised 21 Mar 2015; accepted 22 Mar 2015; published 23 Apr 2015

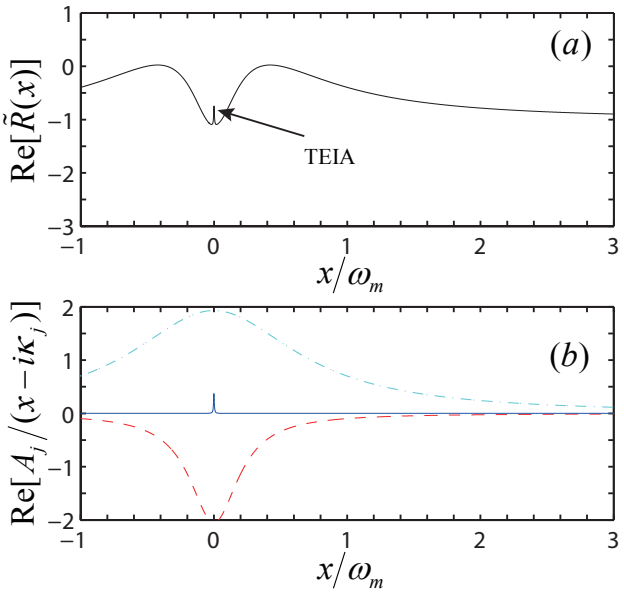

Fig. 4. Same as in Fig. 3, expect for $\lambda = 0.2\omega_m$, $\beta = 0.3{\omega_m}^3$, which corresponds to the black point in area A of Fig. 5. It shows that the optomechanical interaction produces a more sharp TEIA dip within the CRIT window.

response function $\widetilde{R}(x)$. It should be noted that the just mentioned TEIT peak in the transmission spectra manifest themselves as dips here. In this plot, we use the following set of experimentally realizable parameters: $\kappa_c = \omega_m$, $\gamma_m = 10^{-3}\omega_m$, $\kappa_a = 5\gamma_m$. When κ_m is negative, the third term may lead an opposite effect to $\widetilde{R}(x)$, resulting in an absorption dip (similar to before, it is TEIA dip) occurring within the above mentioned CRIT ($\beta = 0$) window, which is shown in Fig. 4(a).

In order to get a criterion to classify TEIT and TEIA, we define $r = \left|\tilde{R}(x=0,\beta,\lambda)\right|^2 \Big/ \left|\tilde{R}(x=0,\beta=0,\lambda)\right|^2$, which means the ratio of transmission at $x = 0$ position between $\beta \neq 0$ and $\beta = 0$ cases. When $r > 1$, a new TEIT peak will emerge on the CRIT peak, while if $r < 1$, there will be a new TEIA dip within there. After few steps of algebra, we find the following inequality from $r < 1$,

$$\frac{1}{\kappa_c + \frac{\lambda^2}{\kappa_a} + \frac{\beta/2\omega_m}{\kappa_m}} > \frac{1}{\kappa_c + \frac{\lambda^2}{\kappa_a}}. \tag{7}$$

Hence, we can obtain the boundary between TEIT and TEIA in the parameter space, which is shown as line b in Fig. 5.

To make sure the TEIT peak or TEIA dip are induced by interference instead of normal modes splitting, such as optomechanical normal-mode splitting [42–44] and coupled-resonators-induced splitting [22], we write Eq. (6) as

$$\widetilde{R}(x) = \frac{A_1}{x - i\kappa_1} + \frac{A_2}{x - i\kappa_2} + \frac{A_3}{x - i\kappa_3} - 1 \tag{8}$$

where κ_j $(j = 1,2,3)$, A_i can be obtained by comparing Eq. (8) with Eq. (6) and solving a cubic equation. The response function $\widetilde{R}(x)$ can be considered as the sum of contributions from the three normal modes formed by coupling the two cavity modes a and c and the mechanical

#234484 - $15.00 USD Received 24 Feb 2015; revised 21 Mar 2015; accepted 22 Mar 2015; published 23 Apr 2015

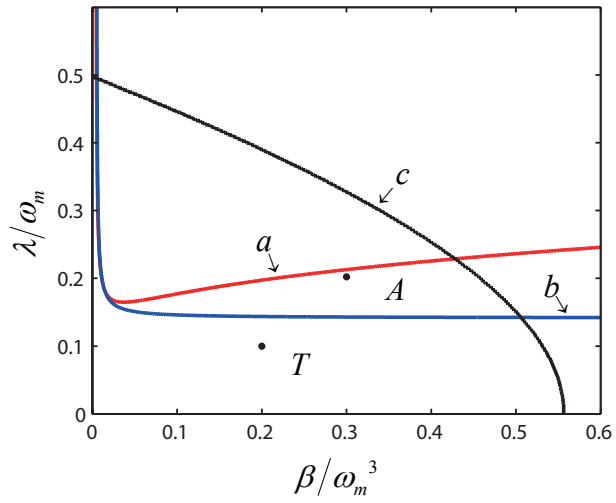

Fig. 5. The phase diagram of TEIT and TEIA. Line a denotes the stability, b denotes the boundary between TEIT and TEIA, and c denotes the boundary of normal-mode splitting. Parameters in the area A encircled by line a, b, and c can lead TEIA, while in the area T encircled by coordinate axis and line a, b, c can lead to TEIT. The other parameters are the same as Fig. 3.

mode b. In Fig. 3(b) and 4(b), we plot these components $A_j/(x-i\kappa_j)$. If κ_1, κ_2, and κ_3 are all real, the three normal modes have the same resonance frequencies and no normal modes splitting occurs. The complicated spectra can only be explained by interference rather than normal mode splitting. In this case, κ_j stands for the linewidth of the three normal modes and the minim κ_j approximately equals to the linewidth of the sharp TEIT peak or TEIA dip. However, if κ_j has a large imaginary part, it implies that the coupling between the three bare modes are too strong, the induced peaks or dips in transmission spectra are roughly the sum of three Lorentzians centered at different frequencies. Therefore, it allows us to give a boundary between TEIT/TEIA and normal mode splitting, which is denoted by line c in Fig. 5. It is shown that if λ and β are beyond a critical value, the normal mode splitting will dominate the transmission spectra.

To get the full boundary for TEIT or TEIA, we have to make sure the above discussion is in the context of stable case. The stable condition can be obtained by calculating the eigenvalues of matrix D as discussed before. In Fig. 5, line a marks out the boundary between the stable and unstable cases. Therefore, we obtain the regime of TEIT and TEIA in parameter space. Parameters in the area A encircled by line a, b, c can lead TEIA dip , while in the area T encircled by coordinate axises and line a, b, c can lead to TEIT peak.

4. Summary

In summary, we proposed a realizable platform to investigate the physics of three-pathway interference. We analyze the physics of the combination of CRIT and OMIT and present detailed calculations. It is shown that in the coupled-cavity system, by introducing optomechanical interaction and a red-detuned driving field, the transmission spectra may emerge sharp TEIT peak or TEIA dip. The lineshape can be easily controlled by adjusting the strength of the cavity coupling, the optomechanical interaction or the pump field. This system may have properties which

#234484 - $15.00 USD Received 24 Feb 2015; revised 21 Mar 2015; accepted 22 Mar 2015; published 23 Apr 2015

are absent in conventional EIT systems, and could be used for measurement or manipulation of optical or mechanical signals in a new way. On the other hand, with this platform, it is possible to obtain a better understanding of coherent phenomena associated with EIT and EIA from a new perspective.

Acknowledgments

This work is supported by the National Natural Science Foundation of China under Grant Nos. 11175094 and 11274197, the National Basic Research Program of China under Grant No. 2011CB9216002.

#234484 - $15.00 USD Received 24 Feb 2015; revised 21 Mar 2015; accepted 22 Mar 2015; published 23 Apr 2015